2

NAVAL POSTGRADUATE SCHOOL

Monterey, California

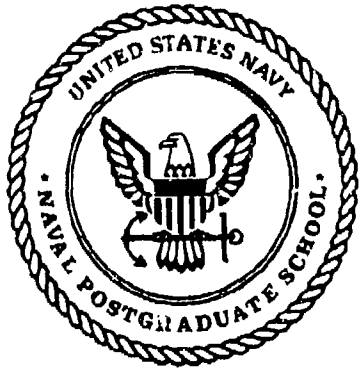

THESIS

PERFORMANCE EVALUATION OF A RADAR BY

COMPUTER

by

Amnauy Thongrod

September, 1992

Thesis Advisor: Gurnam Gill

Approved for public release; distribution is unlimited

548

REPORT DOCUMENTATION PAGE

1a. REPORT SECURITY CLASSIFICATION	1b. RESTRICTIVE MARKINGS
2a. SECURITY CLASSIFICATION AUTHORITY	3. DISTRIBUTION/AVAILABILITY OF REPORT Approved for public release; distribution is unlimited.
2b. DECLASSIFICATION/DOWNGRADING SCHEDULE	
4. PERFORMING ORGANIZATION REPORT NUMBER(S)	5. MONITORING ORGANIZATION REPORT NUMBER(S)
6a. NAME OF PERFORMING ORGANIZATION Naval Postgraduate School 6b. OFFICE SYMBOL (*If applicable*) EW	7a. NAME OF MONITORING ORGANIZATION Naval Postgraduate School
6c. ADDRESS (*City, State, and ZIP Code*) Monterey, CA 93943-5000	7b. ADDRESS (*City, State, and ZIP Code*) Monterey, CA 93943-5000
8a. NAME OF FUNDING/SPONSORING ORGANIZATION 8b. OFFICE SYMBOL (*If applicable*)	9. PROCUREMENT INSTRUMENT IDENTIFICATION NUMBER
8c. ADDRESS (*City, State, and ZIP Code*)	10. SOURCE OF FUNDING NUMBERS Program Element No. / Project No. / Task No. / Work Unit Accession Number

11. TITLE (*Include Security Classification*)
PERFORMANCE EVALUATION OF A RADAR BY COMPUTER (UNCLASSIFIED)

12. PERSONAL AUTHOR(S)

13a. TYPE OF REPORT	13b. TIME COVERED	14. DATE OF REPORT (*year, month, day*)	15. PAGE COUNT
Master's Thesis	From To	September, 1992	53

16. SUPPLEMENTARY NOTATION
The views expressed in this thesis are those of the author and do not reflect the official policy or position of the Department of Defense or the U.S. Government.

17. COSATI CODES			18. SUBJECT TERMS (*continue on reverse if necessary and identify by block number*)
FIELD	GROUP	SUBGROUP	Radar, Performance Evaluation, Performance Methodology

19. ABSTRACT (*continue on reverse if necessary and identify by block number*)

This thesis evaluates the radar range performance of Airport Surveillance Radar (ASR-9) in thermal noise, as well as in presence of clutter and jamming. Radar software available from Artech House was used for the performance evaluation. Computation of detection range in this software is based on empirical calculation of detectability factor in contrast to Marcum-Swerling method which is based on standard radar detection theory. ASR-9 was chosen because it has no military significance and data on it is easily available.

20. DISTRIBUTION/AVAILABILITY OF ABSTRACT	21. ABSTRACT SECURITY CLASSIFICATION	
☒ UNCLASSIFIED/UNLIMITED ☐ SAME AS REPORT ☐ DTIC USERS		
22a. NAME OF RESPONSIBLE INDIVIDUAL Gurnam Gill	22b. TELEPHONE (*Include Area code*) (408) 646-2652	22c. OFFICE SYMBOL EC/GL

DD FORM 1473, 84 MAR — 83 APR edition may be used until exhausted. All other editions are obsolete.

Approved for public release; distribution is unlimited.

Performance Evaluation of a Radar by Computer

by

Amnauy Thongrod
Lieutenant, Royal Thai Navy
B.S., Royal Thai Naval Academy

Submitted in partial fulfillment
of the requirements for the degree of

MASTER OF SCIENCE IN SYSTEM ENGINEERING

from the

NAVAL POSTGRADUATE SCHOOL
September 1992

Author: Amnauy Thongrod
Amnauy Thongrod

Approved by: G. S. Gill
Gurnam Gill, Thesis Advisor

David C. Jenn
David C. Jenn, Second Reader

Jeffrey Knorr, Chairman
Electronic Warfare Academic Group

ABSTRACT

This thesis evaluates the radar range performance of Airport surveillance Radar-(ASR-9) in thermal noise, as well as in presence of clutter and jamming. Radar software available from Artech House was used for the performance evaluation. Computation of detection range in this software is based on empirical calculation of detectability factor in contrast to Marcum-Swerling method which is based on standard radar detection theory. ASR-9 was chosen because it has no military significance and data on it is easily available.

TABLE OF CONTENTS

ACKNOWLEDGMENTS

I am deeply indebted to Dr. Gurnam Gill, my thesis adviser for all the encouragement to complete this thesis. Under his guidance I was able to get better understanding of radar systems. I would like to thank Professor David C. Jenn, who had taught me the first course about radar, and also has reviewed this work.

Finally, I thank all the staff of Naval Postgraduate School for the encouragement given to me during the course of my education at this great institution.

I. INTRODUCTION

It takes several years and a large amount of money to develop radar related weapon systems. Radar performance evaluation methods play a vital role in risk reduction of these costly development and procurement programs. In the early stages of development, when no hardware is available, radar performance evaluation is made by analysis and simulation using the performance evaluation tools. Radar design is reiterated until it satisfies the desired requirements. These performance evaluation tools are also used by government agencies to perform comparative evaluations of various system designs offered by competing contractors. In the later stages of radar development, when hardware becomes available, performance evaluation is performed by laboratory tests and field tests. Computerized performance evaluation can still be used to expand the envelope of field tests. This is desirable as it will reduce the overall cost of testing as exhaustive field tests are expensive to carry out.

Radar evaluation is normally made in several steps, depending on the status of the program and the resources available to the evaluator. The necessary analysis may start from fundamental theoretical models of radar performance, or from available test data on similar radar equipment which may need to be improved to meet the new requirements. Some areas of radar performance are well understood,

and accurate calculations of system performance can be made from the known radar parameters and the models of the external environment in which the radar is intended to operate.

In other cases, reliable theoretical procedures which permit accurate prediction of radar performance have not been developed, and simulation or field test will be required. Even in those areas where adequate theory exists, there still remains considerable uncertainty as to the validity of models used to represent target and environmental effects, and key aspects of performance can only be validated by tests. A thorough analytical evaluation is required, however, to identify the specific critical areas in which tests are necessary to resolve existing uncertainties.

The need for analytical evaluation prior to testing is based on the limited test resource available and on the statistical nature of most radar performance measures. Analysis techniques are seldom reliable enough to permit a positive decision on the radar production without validation through actual field tests. On the other hand, radar designs which have fundamental flaws or limitations can often be rejected on the basis of analysis alone. When particular areas of concern are identified by analysis, it is usually possible to design test programs to determine whether these areas are adequately addressed by radar design.

In this thesis, performance of an existing air surveillance radar (ASR-9), will be evaluated using the 'Radar Evaluation Software' which is commercially available

from Artech House. General characteristics of ASR-9 are described in Chapter II. The required theoretical background for performance evaluation is given in Chapter III. In Chapter IV the results of radar performance is presented.

II. RADAR DESCRIPTION

A. AIR SURVEILLANCE RADAR

Originally, primary radars were magnetron systems equipped with a single fan-beam antenna mounted on an azimuth rotator. Later versions incorporated moving target indicator (MTI) detectors, which used delay lines to cancel ground clutter. Even MTI radars had difficulty in the detection of low altitude aircraft in the presence of ground vehicles, rain, and other interference. To handle such adverse conditions, the Air Surveillance Radar (ASR-9), a present generation primary airport radar, uses the Moving Target Detector (MTD) concept. MTD employs several adaptive digital signal and data processing techniques. For example, doppler processing eliminates ground and rain clutter which is followed by a number of target editing steps; e.g., a ground-clutter map rejects false alarms that result from mountains and buildings. Fixed and area (adaptive) thresholds are used to eliminate echoes caused by flocks of birds or unwanted targets such as automobiles and trucks. MTD achieves further reduction of false alarms with a surveillance-processing module that uses scan-to-scan correlation for rejecting targets that fail to meet spatial or temporal criteria. As a result, ASR-9 can deliver

reports free from clutter and false alarms found in earlier airport primary radars. MTD processing is explained in subsequent paragraphs.

Figure 1 shows a block diagram of the MTD system, which includes a dual fan-beam elevation antenna.

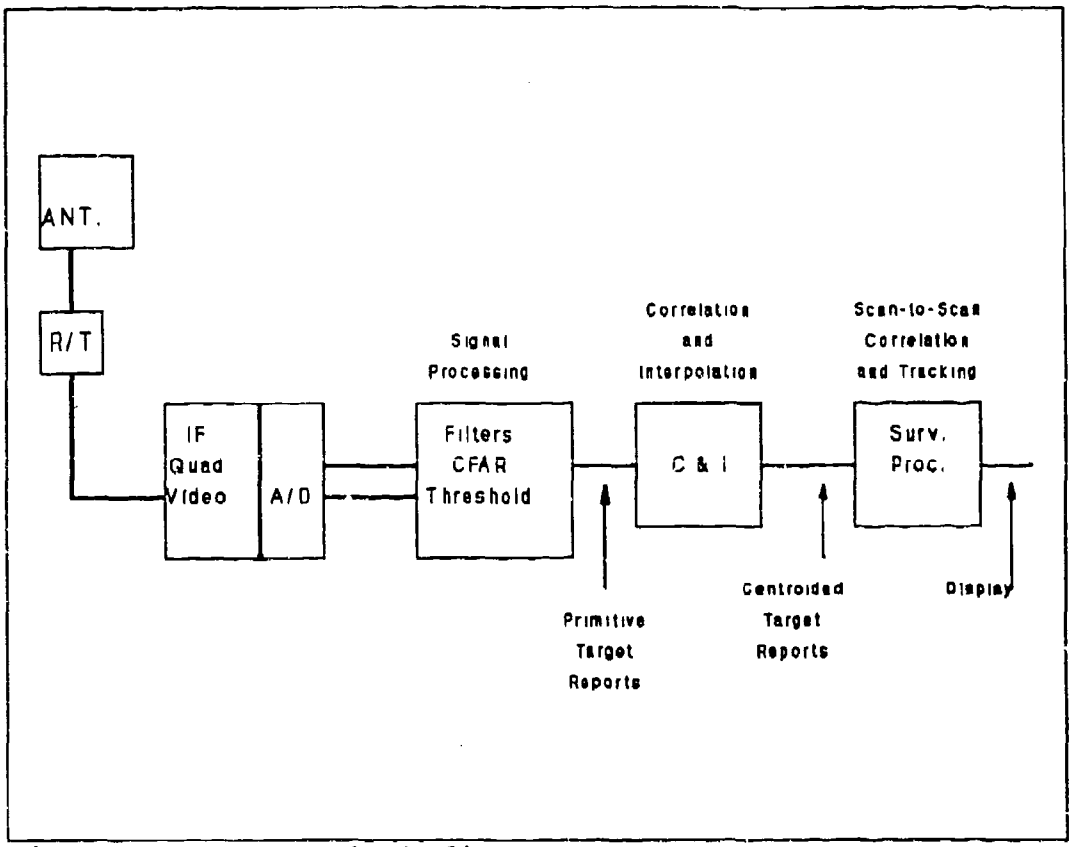

Figure 1. MTD-II Block diagram

The upper beam is used for close range targets and it receives a smaller amount of ground clutter. The lower beam is used for distant targets; its minus 3-dB point is typically directed toward the horizon.

The antenna normally both radiates and receives vertical polarization. However, when there is heavy precipitation over a significant portion of coverage area, the radar switches to circular polarization. By doing so, the sensor achieves an additional 12 to 20 dB of precipitation-echo rejection. During the time that circular polarization is used, weather signals are derived from the orthogonal-polarization ports of the antenna. Meanwhile, the target signals are received through the same ports of the antenna that are used when linear polarization is radiated. Multiple-channel rotary joints carry the information of the received signals to the processing units, which are located in a shelter at the base of antenna tower. During operation with circular polarization, a switch located on the antenna selects either the weather-channel upper or lower beam. The signal from the selected beam is then passed through a single rotating joint to the weather-channel receiver.

Signals for target detection pass from the antenna through a sensitivity time control and a low-noise amplifier. Signals are then heterodyned to an intermediate frequency, and translated to baseband at the output of the receiver to provide in phase and quadrature video signals. A/D converters sample these in-phase and quadrature (I-Q) video channels to generate digital output for further processing.

There are two coherent processing intervals (CPI) for each beam dwell, and each beam dwell commences in synchronism with a bearing pulse from the shaft encoder that reports the antenna's position. In the case of ASR-9, the individual

CPIs in the CPI pair use 8 and 10 pulses, respectively, with a nominal average pulse-repetition frequency (PRF) of 1,000 Hz and nine-to-seven ratio between the two CPIs. Fill pulses account for variations in the angular rate of the antenna that result from wind effects.

For each of the 8 or 10 CPI periods, the processor's input memories store the signals for the 960 range gates, which span 60 nmi with a range resolution of 1/16 nmi. The processor then performs saturation and interference testing of the digital signals, followed by doppler filtering and thresholding. Finally, range, azimuth, Doppler amplitude, and quality values are delivered for the targets in the range cells that contain detections. (A quality value indicates the expected azimuth estimate error.) The detections are then correlated and centroids are found for the range and azimuth measurements. Reports are then subjected to additional criteria for false-alarm rejection, before passing on to a scan-to-scan correlator that reduces the output false-alarm rate to about one per scan.

B. THE MTD PROCESSOR

The MTD process performs several functions such as signal processing, thresholding, area thresholding and scan-to-scan correlation.

1. Signal Processing

MTD's central functional element is a set of doppler filters, typically 8 or 10 for each range cell. The output of the filters are all individually subjected to thresholds. The input to the filters is derived from the output of the quadrature video detectors. which are sampled by two 12-bit A/D converters operating at a rate of 1 MHz. For each 4.8 second revolution of radar antenna, there are 256 azimuth beam dwells, each of which contains two CPIs. For each CPI, 960 range cells are processed. Thus, after every revolution of the antenna, more than 4 million doppler filters are formed.

The output of doppler filters is examined by the signal processor, which uses threshold criteria appropriate to the desired false-alarm rate and to the locations of the signals relative to several factors: ground clutter, precipitation echoes, and the number of bird echoes encountered. Two pulse-repetition intervals are used to prevent the masking due to blind speed and the masking that occurs when rain clutter obscures a target.

2. Thresholding

The signal will be declared as the target if and only if it exceeds a certain threshold. The threshold in the case of the zero velocity filter is established from the average of 10-20 scans. A double sided sliding-window, constant false-alarm rate (CFAR) threshold is used to determine the range thresholds for nonzero-

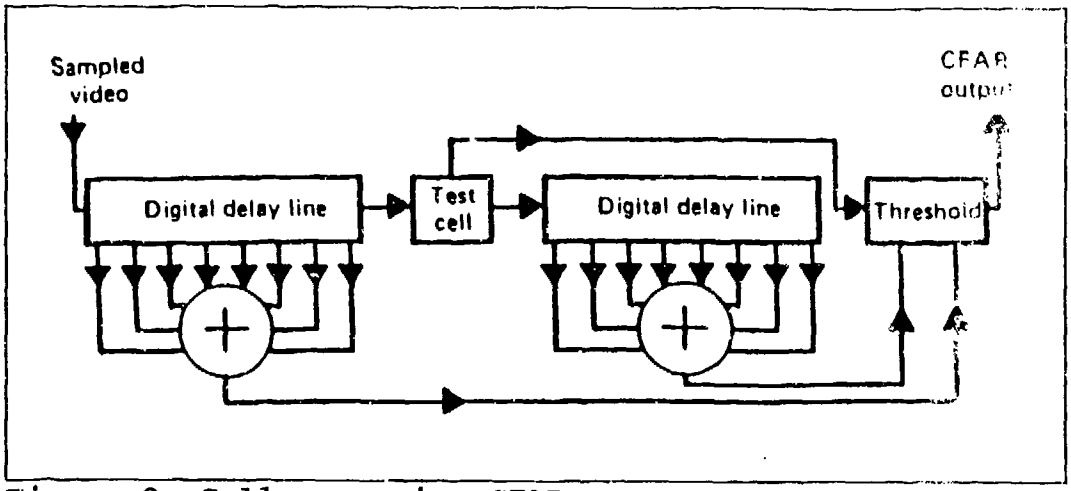

Figure 2 Cell-averaging CFAR

doppler-velocity filters. The CFAR processor calculates a threshold by averaging the eight cells preceding and eight cells following an interval that includes the range cell under test (Thus the total window, which is approximately 1 nmi long, includes 16 range cells). The main objective of CFAR is to adjust the threshold so that the false alarm rate is maintained constant. To improve resolution, ASR-9 uses the algorithm that does not consider the first three strongest echoes within the CFAR window. Thus it can resolve the target as close as 0.25 nmi.

3. Post-Detection Processing

In post-detection processing, threshold target reports are subjected to additional filtering. This filtering removes ground clutter that exceeds the design characteristics of the filter bank. A high-spatial-resolution map (0.25 nmi x 2.8^0) is employed to select the appropriate threshold values for the ground clutter; a doppler weighting that corresponds to the scanning modulation and, for the ground

traffic, a flat-topped Doppler weighting. After this operation is completed, the reports are correlated and interpolated. Targets are grouped in accordance with their spatial adjacency. The centroids of the different groups are then calculated from a center-of-mass estimation (first moment weighted by amplitude). Each centroided target report is given a quality value:an integer ranging from 0 to 3 that indicates the number of detections that were made as the antenna scanned past the target. A high quality value corresponds to a greater number of detections. The MTD tracker uses a target's quality value as one of the criteria in deciding whether the target should be ignored, entered to update a track, or pursued to initiate a new track during the next scan. The ASR-9 design enhances azimuth resolution by employing a beam-matching algorithm. When a run of reports extends beyond two beamwidths, ASR-9 compares the amplitude data with a pattern that a large single target would produce. A substantial difference between the amplitude data and the expected pattern implies the existence of two targets in close azimuthal proximity.

4. Area Thresholding

The sensitivity of MTD-II permits the detection of birds and insect targets that have mean cross sections of approximately 0.003 m^2 and effective radar-backscattering cross sections as small as 0.001 m^2. In comparison, aircraft targets have apparent mean cross sections of 1 m^2. The area-thresholding process reduces the effects of bird populations by limiting the false alarm rate to a fixed

maximum value that has as small an effect on the detection rate as possible. The threshold is set by integrating reports for the time necessary to obtain an accurate estimate of low cross-section target detections. If the count exceeds a nominal value of 60 false alarms per scan over the coverage area, the area-thresholding processor raises the thresholds. To overcome the flocks of bird clutter, area-thresholding uses two filters. The first filter integrates over 200 seconds with approximately 16 mi^2 x 3-Doppler-bin resolution. The second filter integrates over 5 seconds and covers within 20 miles of radar and within 3 Doppler bins. The two-filter combination mitigates, on a localized basis, the effects of long lasting bird flights. At the same time, the filter combination can respond quickly to cope with the sudden flight of a flock of birds.

5. Scan-to-Scan Correlation (Tracking)

The target is subjected to additional filtering after it passes through the area thresholding. This filter will select the target which correlates with the target from the previous scan and then predict the next position on this basis. If the true target in the next scan does not appear at the expected position (within some allowable error), that target will be dropped after three consecutive scans. MTD also drops targets that correlate with track but never move more than 0.25 mi from an initial position.

6. Elimination of Ambiguous Range

The pulse repetition intervals are staggered using microstagger, which increases the pulse-repetition interval by two range cells (approximately 300 m) so that echoes from the ambiguous-range intervals are asynchronous with one another. Using this asynchronism, the range-ambiguous echoes of the target are eliminated. However, in mountainous regions where range-ambiguous clutter can occur, it is necessary to revert to a nonstaggered pulse-repetition interval in order to eliminate the clutter.

7. Moving Ground Targets

Subclutter visibility of ASR-9 is of the order of 45 dB. Even in heavy clutter within the range cell, this radar still can detect the target. On the other hand, this could be a critical problem for the surveillance radar because the automobile moving with the velocity comparable to the aircraft can be easily detected by the MTI radar. This problem is fixed by taking advantage of the vertical-interferometer effect: the phase of a ground target is different from that of an air target echo.

C. RADAR PARAMETERS

Transmitter

Peak Power (at coupler)	1.12 MW
Pulse Width (3dB)	1.03 μs

Radiated Frequency	2.7-2.9 GHz	
Transmission Line Loss	1.0 dB	
Receiver		
Noise Figure (max)	4.1 dB	
Transmission Line Loss	1.6 dB	
Mismatch and Range Sampling Loss (C_b)		1.0 dB
Sensitivity (min)		-108 dBm
Antenna		
Power Gain		
Low Beam		34 dB
High Beam		33 dB
Azimuth Beamwidth,Both Beams (3dB)		1.4 deg
Elevation Beamwidth (3dB)		4.8 min
Rotation Rate (RPM)		12.5±10%
Signal Processor		
No.of Filters in Low PRF		8
No.of Filters in high PRF		10
Pulses in Low PRF CPI		8
Pulses in High PRF CPI		10
Average Coherent Integration Gain		8.25 dB

Signal Processing Losses(L_x)	3.25 dB
PRF	928 to 1321 Hz

ASR-9 has been approved by the FAA as it meets most of the requirements of a primary radar for the airport. It meets the requirement of range detection, probability of detection and false alarm rate, range resolution, angle resolution and traffic handling capacity. Weather channel specifications are not discussed here because it is beyond the scope of this study. Some techniques mentioned in this section are not only used in the civilian radars, but also widely used in most of the military radars. Since most of the design details of ASR-9 are unclassified and readily available this radar is chosen as the subject of the performance evaluation instead of a military radar.

III. PERFORMANCE EVALUATION METHODOLOGY

A. PERFORMANCE METHODOLOGY

Radar evaluation is normally done in several steps and typically follows the sequence given below

1. Analysis and Simulation;

2. Subsystem tests;

3. Laboratory tests;

4. Field tests; and

5. Extrapolation from tests, using analysis, simulation and field test results. However, we will only evaluate radar performance by using analysis in this thesis.

Marcum-Swerling developed the radar detection theory for five kinds of target models. However these computations are complex and time consuming. Barton developed an empirical method to solve the radar detection problem. All the detectability equations in this section are empirical in nature and may not be justified by exact theoretical analysis.

In a typical calculation, maximum target detection range is computed for given probability of detection P_d, probability of false alarm P_{fa}, target model and the radar system parameters. The above computation assumes a target signal in the

presence of thermal noise. The procedure is then extended to the determination of target detection range in the presence of jamming and surface clutter.

B. DETECTION RANGE IN THERMAL NOISE

In Barton's procedure [Ref.2] the detectability factor D_x plays a central role in the computation which is defined later in this section. Once the detectability factor is computed, the detection range is computed from

$$R_m^4 = \frac{P_t \tau G_t G_r \lambda^2 \sigma F_r^4}{(4\pi)^3 D_x k T_s L_t L_a} \qquad (3.1)$$

where

P_t is peak power

τ is pulse width

G_t, G_r is gain of transmitter and receiver antennas

σ is radar cross section of target

F_r^4 is pattern propagation factor

k is boltzmann's constant

T_s is system temperature

L_α is attenuation loss

L_t is transmission line loss

The effective detectability factor (D_x) is defined as the required signal-to-noise ratio to achieve particular probabilities of detection and false alarm for a specific target model. It also includes receiver matching loss , beamshape loss , and the signal processing loss. D_x can be written as

$$D_x = D_x(n)\, M L_p L_x = \frac{E_1}{N_o} \qquad (3.2)$$

where

x indicates target model. x will be 0,1,2,3,4 referring to Swerling target model

n is the number of pulses integrated

L_x is signal processing loss that consists of eclipsing loss, straddling loss, velocity response loss and CFAR loss

L_p is beamshape loss

M is receiver matching loss

$D_x(n)$ is signal-to-noise ratio (SNR) required to produce P_d and P_{fa} when n pulses are noncoherently integrated and target RCS model is Swerling x

E_1 is the signal energy

N_o is noise spectral density

$D_x(n)$ in equation 3.2 is determined from

$$D_x(n) = \frac{D_0(1)\, L_i(n)\, L_f(Kn_e)}{n} \qquad (3.3)$$

where $L_i(n)$ is the integration loss when n pulses are integrated for any target model x (0,1,2,3,4). The integration loss is zero for ideal coherent integration. $L_i(n)$ is defined as

$$L_i(n) = n\, D_0(n)/D_0(1)$$

where $D_0(1)$ is single pulse SNR for a constant target to achieve particular P_d and P_{fa}. The value of $D_0(1)$ may be obtained from Figure 4, but it is also available in radar evaluation software. $D_0(n)$ is the required SNR for each pulse of the n-pulse train. Plots of $L_i(n)$ for various $D_0(1)$ are shown in Figure 3. It should be noted that $L_i(n)$ is same for all target models.

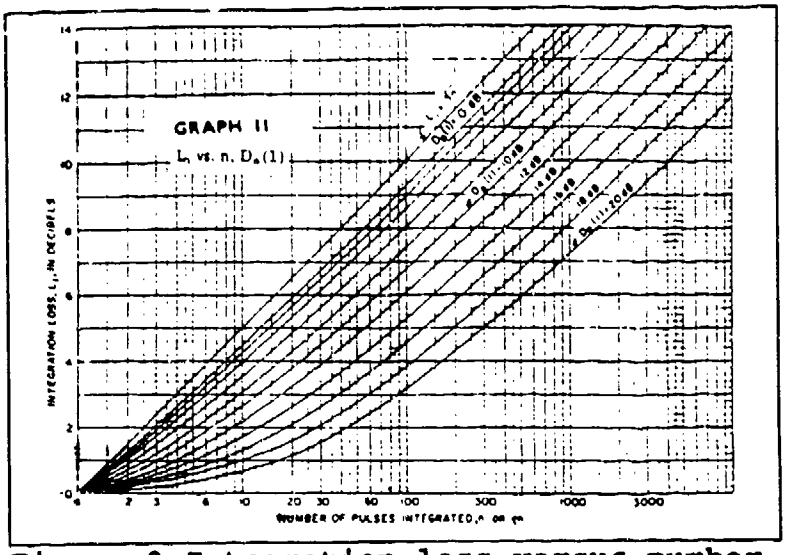

Figure 3 Integration loss versus number of pulses integrated after envelope detection

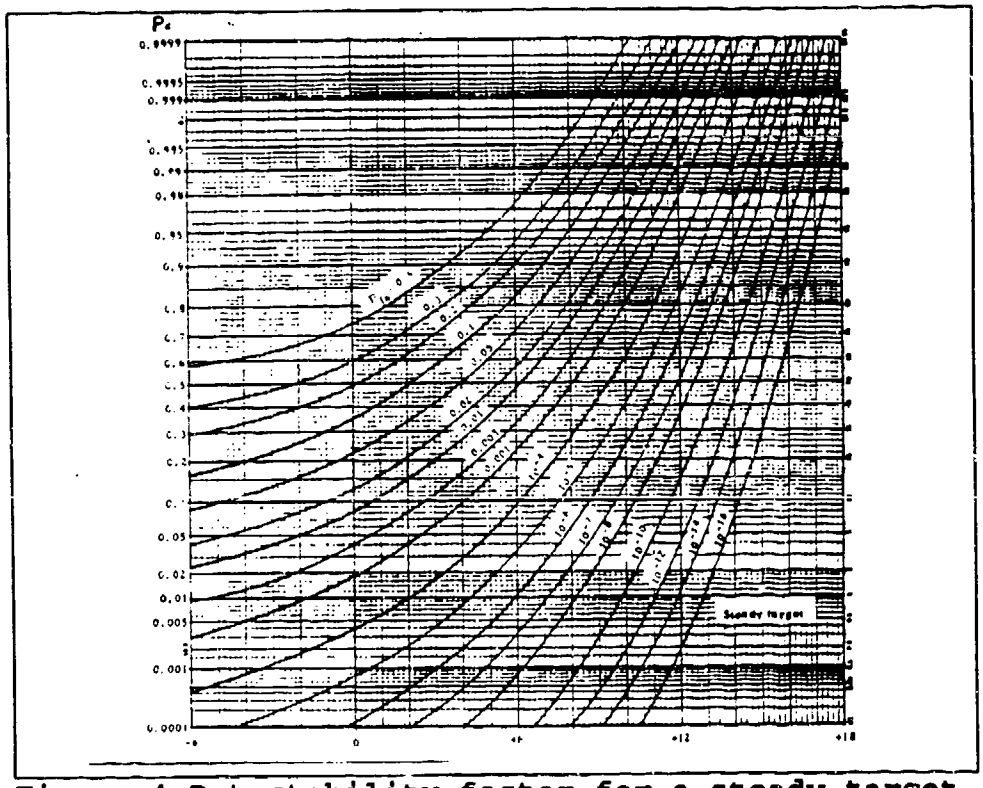

Figure 4 Detectability factor for a steady target

However $L_f(Kn_e)$ in (3.3), the loss due to the fluctuation of target radar cross section is computed separately for each target model. This loss for general case target model is defined as

$$L_f(Kn_e)\ dB = \left(\frac{1}{Kn_e}\right) L_f(1)\ dB \qquad (3.4)$$

where

K is the half number of independent Gaussian components

n_e is the number of independent signals integrated during n pulses

Values of n_e and K are given by

case 0 (steady target)	$n_e \rightarrow \infty$, $K \rightarrow \infty$
case 1	$n_e = 1$, $K = 1$
case 2	$n_e = n$, $K = 1$
case 3	$n_e = 2$, $K = 2$
case 4	$n_e = 2n$, $K = 2$

$L_f(1)$ in (3.4) is a fluctuation loss for case 1 target model. This loss, plotted in Figure 5 for single-pulse case, is primarily a function of P_d, but also depends weakly on P_{fa}.

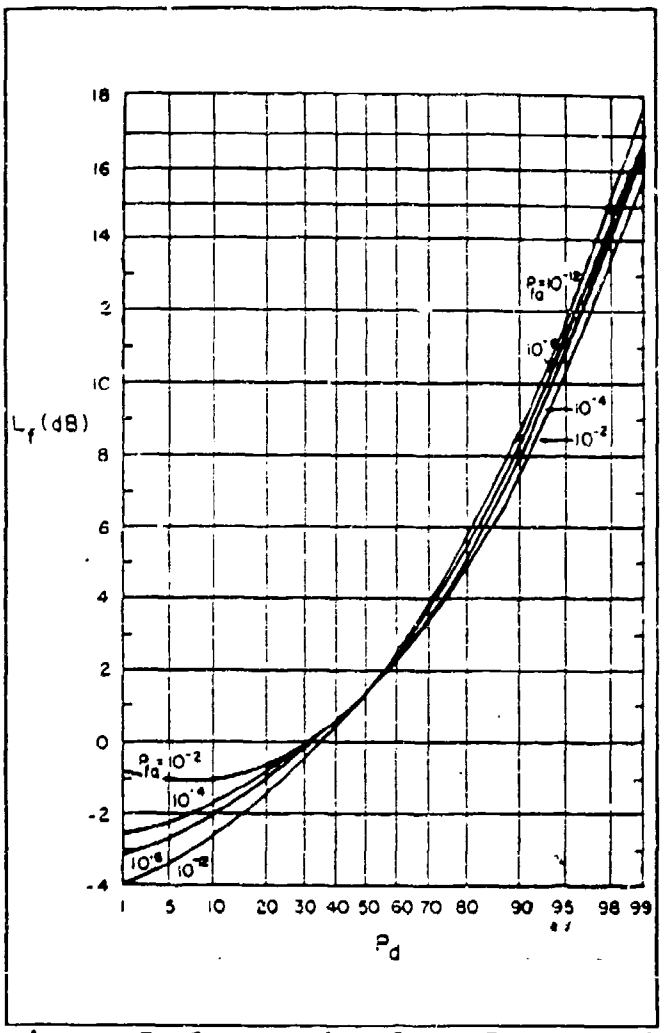

Figure 5 Fluctuation loss for case 1 target

System noise temperature (T_s) can be used to define the noise environment. Using the method of Blake, system noise temperature (T_s) may be divided into three major components

$$T_s = T_a + T_r + L_r T_e$$

where

$$T_a = \frac{0.88 T_a' - 254}{L_a} + 290$$

$$T_r = T_{tr} (L_r - 1)$$

$$T_e = T_o (NF - 1)$$

T_a is antenna noise temperature (°K)

T_a' is the apparent temperature of sky as viewed at the radar frequency[Ref.2:pp.15].

L_a is antenna dissipative loss

T_r is receiver line noise temperature

T_{tr} is physical temperature of transmission line

L_r is receiver line loss

T_e is receiver noise temperature

T_o is reference temperature

NF is receiver noise figure

Others parameters in (3.1) are obtained from the radar specification. There may be several slightly different procedures to compute radar range detection.

C. DETECTION RANGE IN THE PRESENCE OF JAMMING

Noise jammers are often used to degrade the performance of surveillance radar. Noise jamming degrades the victim radar by raising the noise level in its receiver. In the radar evaluation software, jamming is represented by its equivalent temperature which is derived below.

Jamming power into the radar is given by

$$J = \frac{P_j G_j G_r \lambda^2 F_j^2}{(4\pi)^2 R_j^2 L_{\alpha_j}} \times \frac{B_r}{B_j} \qquad (3.5)$$

where

P_j is jammer power

G_j is gain of jammer antenna

F_j is pattern propagation factor from the jammer into the radar antenna

R_j is range to the jammer

$L_{\alpha j}$ is the one-way atmospheric attenuation

B_r is radar receiver bandwidth

B_j is jammer receiver bandwidth

Jammer spectral density at the radar receiver is written as

$$J_o = \frac{J}{B_r} \qquad (3.6)$$

Jammer equivalent temperature is given by

$$T_j = \frac{J_o}{k} \qquad (3.7)$$

Combining equations 3.5, 3.6, and 3.7, the T_j can be written as

$$T_j = \frac{P_j G_j G_r \lambda^2 F_j^2}{(4\pi)^2 k B_j R_j^2 L_{a_j}} \qquad (3.8)$$

With jamming the system temperature has gone up from T_s to T_s+T_j. The new detection range is given by

$$R_m^4 = \frac{P_t \tau G_t G_r \lambda^2 \sigma F_r^4}{(4\pi)^3 D_x k (T_s+T_j) L_t L_a} \qquad (3.9)$$

For two or more jammers, individual values of T_{ji} are calculated, and the total system temperature is the sum of $T_s+T_{j1}+T_{j2}+.....$

D. DETECTION RANGE IN CLUTTER

Radar clutter is defined as unwanted echoes from the ground, sea, rain, chaff, birds and insects. Clutter reflectivity as viewed by a ground radar is the product of two factors: $\sigma^o F_c^4$ where σ^o is surface clutter reflectivity, and F_c is pattern propagation factor in clutter.

Using the radar range equation the power spectral density of the clutter return is given by

$$C=\frac{P_t\tau G_t G_r \lambda^2 \sigma_c F_c^4}{(4\pi)^3 R_c^4 L_t L_{a_c}} \qquad (3.10)$$

where

$$\sigma_c = \sigma^o A_c$$

$$A_c = \left(\frac{R_c \theta_a}{L_p}\right)\left(\frac{\tau C}{2}\right)\sec(\psi)$$

$$\sigma^o = \gamma \sin(\psi)$$

$$\sin\psi = h_r/R_c$$

Variables in above equations are defined as

σ_c is clutter cross section

A_c is area of surface within the radar resolution

θ_a is azimuth beamwidth

C is velocity of propagation of light

ψ is grazing angle (For a ground radar, ψ is generally small, hence $\sec\psi \approx 1$.)

γ is proportionality constant, it has a value from 0.03 to 0.15

h_r is antenna height

R_c is clutter range

Clutter cross-section for a ground-based radar is

$$\sigma_c = \frac{\gamma h_r}{R_c} \left(\frac{R_c \theta_a}{L_p}\right) \left(\frac{\tau C}{2}\right) \qquad (3.11)$$

Substituting the expression for σ_c in equation 3.10

$$C = \frac{P_t \tau G_t G_r \lambda^2 \sigma_c F_c^4}{(4\pi)^3 R_c^4 L_t L_{a_c}} \gamma \frac{h_r}{R_c} \left(\frac{R_c \theta_a}{L_p}\right) \left(\frac{\tau C}{2}\right) \qquad (3.12)$$

The power spectral density of the target return is

$$S = \frac{P_t \tau G_t G_r \lambda^2 \sigma F_r^4}{(4\pi)^3 R^4 L_t L_a} \qquad (3.13)$$

From equations 3.12 and 3.13, the signal-to-noise ratio for a target in a background of surface clutter is

$$\frac{S}{C} = \frac{\sigma F_r^4 L_p R_c^4 L_{a_c}}{R^4 h_r \theta_a \left(\frac{\tau C}{2}\right) L_a \gamma F_c^4} \qquad (3.14)$$

S/C depends heavily on the pattern propagation factor F_c which is defined for three different ranges as given below

1. Short Range, $R < R_1$

   where $R_1 = 4\pi h_t \sigma_h / \lambda$

   σ_h in the above expression is the RMS value of surface roughness

   Pattern propagation factor for this range is

   $$F_c^4 \approx 1$$

2. Medium Range, $R_l < R < R_h$

$$F_c^4 \approx (R_l/R)^4$$

3. Long Range $R > R_h$ (Diffraction region)

where $R_h = 4130\ h_r^{0.5}$

In this region, F_c can be calculated by using the elaborate analytical approximation given in Ref.2:pp 553-558.

The signal-to-clutter ratio at the output of the clutter canceler can be written as

$$\left(\frac{S}{C}\right)_o = I_m \frac{S}{C} \qquad (3.15)$$

From equation 3.14 and 3.15

$$\left(\frac{S}{C}\right)_o = \frac{I_m \sigma F^4 L_p R_c^4 L_{a_o}}{R^4 h_r \theta_a \left(\frac{\tau c}{2}\right) L_a \gamma F_c^4} \qquad (3.16)$$

From the above equation, the maximum detection range can be written as

$$R_m^4 = \frac{I_m \sigma F^4 L_p R_c^4 L_{a_o}}{\left(\frac{S}{C}\right)_o h_r \theta_a \left(\frac{\tau c}{2}\right) L_a \gamma F_c^4} \qquad (3.17)$$

In the software $(S/C)_o$ is termed the detectability factor for detection in clutter. Theoretical background of the performance evaluation software has been discussed in this section. The results of the performance evaluation will be presented in the next chapter.

IV. PERFORMANCE EVALUATION

A radar performance evaluation is presented in this chapter. The results are obtained using computer software. The theoretical basis of the software has been presented in Chapter III.

A. DETECTION RANGE IN THERMAL NOISE

Using the radar evaluation software, data in Table 1 were generated. This table shows detection ranges and detectability factor for various P_d (for a fixed P_{fa} of 10^{-6})and target models. R_0, R_1, R_2, R_3 and R_4 in Table 1 denote detection range for the five target models.

Radar parameters from Chapter II were used as inputs to the program. The program requires additional data on target RCS, target height and the nature of ground terrain. A target RCS of 1 m^2 and height of 1 km were assumed. Ground terrain was assumed to be 'smooth'.

Data from Table 1 is plotted in Figure 6 as P_d versus detection range. The results are in agreement with the radar detection theory. It is clear from Figure 6 that the constant RCS target model gives a longer detection range as compared to other target models when P_d is greater than 0.3.

Table 1. DETECTION RANGE IN THERMAL NOISE VS DETECTABILITY

Target models	Constant target		SW.1 target		SW.2 target		SW.3 target		SW.4 target	
P_d	Dx (dB)	R_0 (km)	Dx (dB)	R_1 (km)	Dx (dB)	R_2 (km)	Dx (dB)	R_3 (km)	Dx (dB)	R_4 (km)
0.1	8.96	112.2	7.23	122.1	8.74	113.4	8.53	114.6	8.91	112.5
0.3	10.49	104.0	10.39	104.5	10.47	104.1	10.46	104.2	10.48	104.1
0.5	11.56	98.6	13.11	91.2	11.75	97.7	11.95	96.7	11.61	98.4
0.7	12.83	92.5	16.58	76.4	13.30	90.3	13.77	88.2	12.95	92.0
0.8	13.83	87.9	19.22	66.6	14.5	85.0	15.18	82.1	14.0	87.2
0.9	15.75	79.7	23.9	51.7	16.77	75.6	17.79	71.7	16.01	78.7

Dx: Detectability factor

R's: Maximum radar detection range

SW.'s: Swerling target models

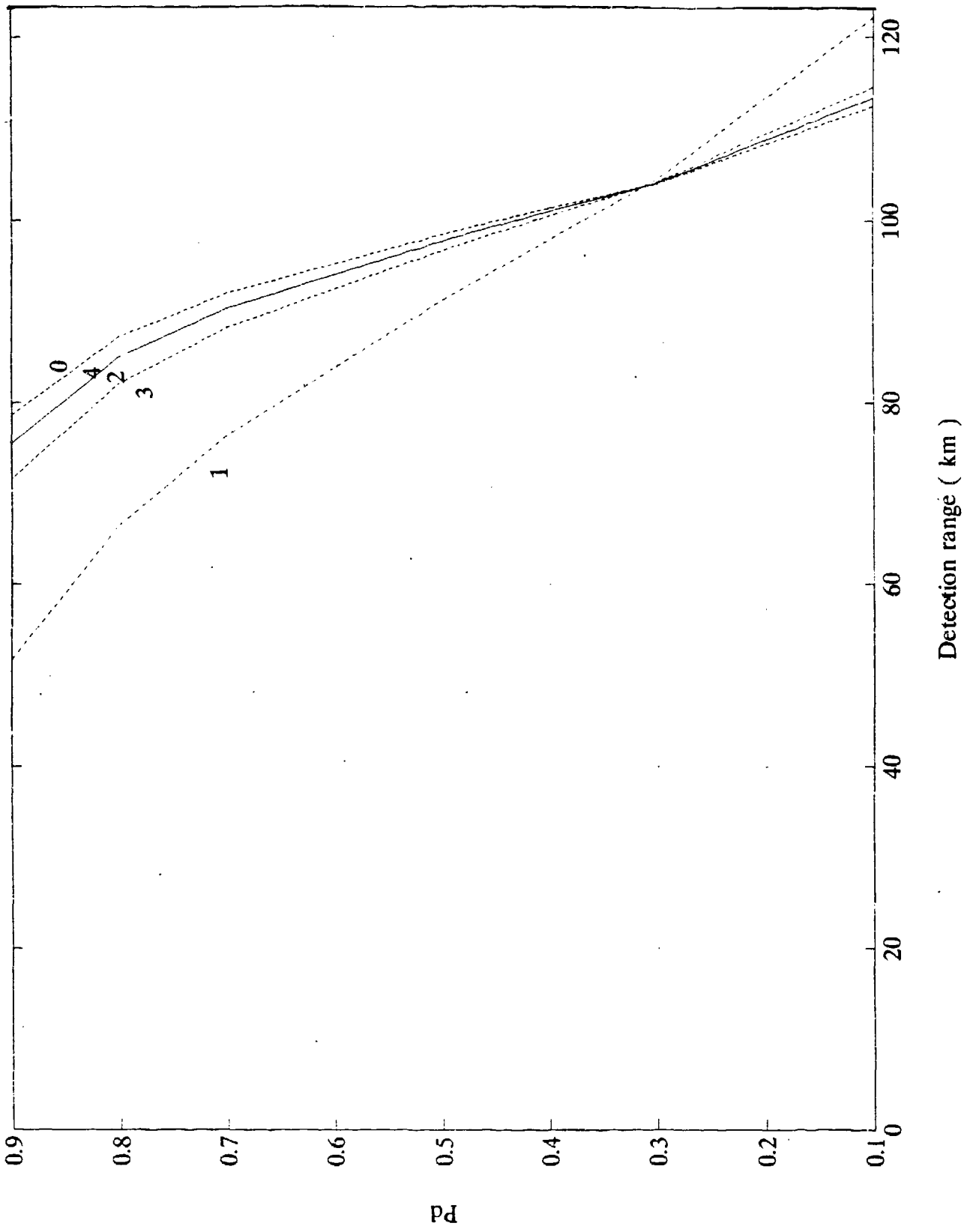

Figure 6 Detection range performance in Thermal noise for different Swerling target models

B. DETECTION RANGE IN THE PRESENCE OF STAND OFF JAMMING

Evaluation of radar performance in the presence of stand off jammer (SOJ) is an extension of radar performance in thermal noise. Jamming power is converted into an equivalent noise temperature and later combined with the system noise temperature (T_s). SOJ is assumed to be at a distance of 380 km from the radar and it is jamming the radar through the main lobe.

The jammer parameters are as follows

Jammer range from Radar	380	km
SOJ azimuth from Radar	0	deg
SOJ altitude above Earth's surface	8.135	km
Jammer ERP (P_jG_j)	10	kw
Jammer bandwidth	300	Mhz
Jammer polarization	Vertical	
Jammer noise quality (Q)	0	dB

Software (module 'Detection range in jamming') was used to determine the effect of stand off jammer on ASR-9. The last column in Table 2 shows the signal to interference ratio (SIR) for constant radar cross section target at various ranges. It is apparent from the table that SIR decreases quickly as target range increases.

Table 2. SIGNAL-TO-JAMMING PLUS NOISE VS TARGET RANGE

Range	J_o/N_o	N_o	J_o	I_o	I_o/N_o	E/N	SIR (dB)
22.0	18.94	-199.3	-180.3	-178.8	20.5	36.92	16.5
43.0	18.94	-199.3	-180.3	-180.2	19.1	27.31	8.2
64.0	18.94	-199.3	-180.3	-180.3	19.0	20.07	1.0
85.1	18.94	-199.3	-180.0	-180.3	19.0	14.60	-4.4
106.1	18.94	-199.3	-180.3	-180.3	19.0	10.22	-8.8
127.1	18.94	-199.3	-180.3	-180.3	19.0	6.52	-12.5
148.1	18.94	-199.3	-180.3	-180.3	19.0	-34.20	-53.2
169.1	18.94	-199.3	-180.3	-178.0	21.3	-90.73	-112.0
190.2	18.94	-199.3	-180.3	-180.1	19.2	-147.10	-166.3
211.2	18.94	-199.3	-180.3	-180.3	19.0	-203.37	-222.4

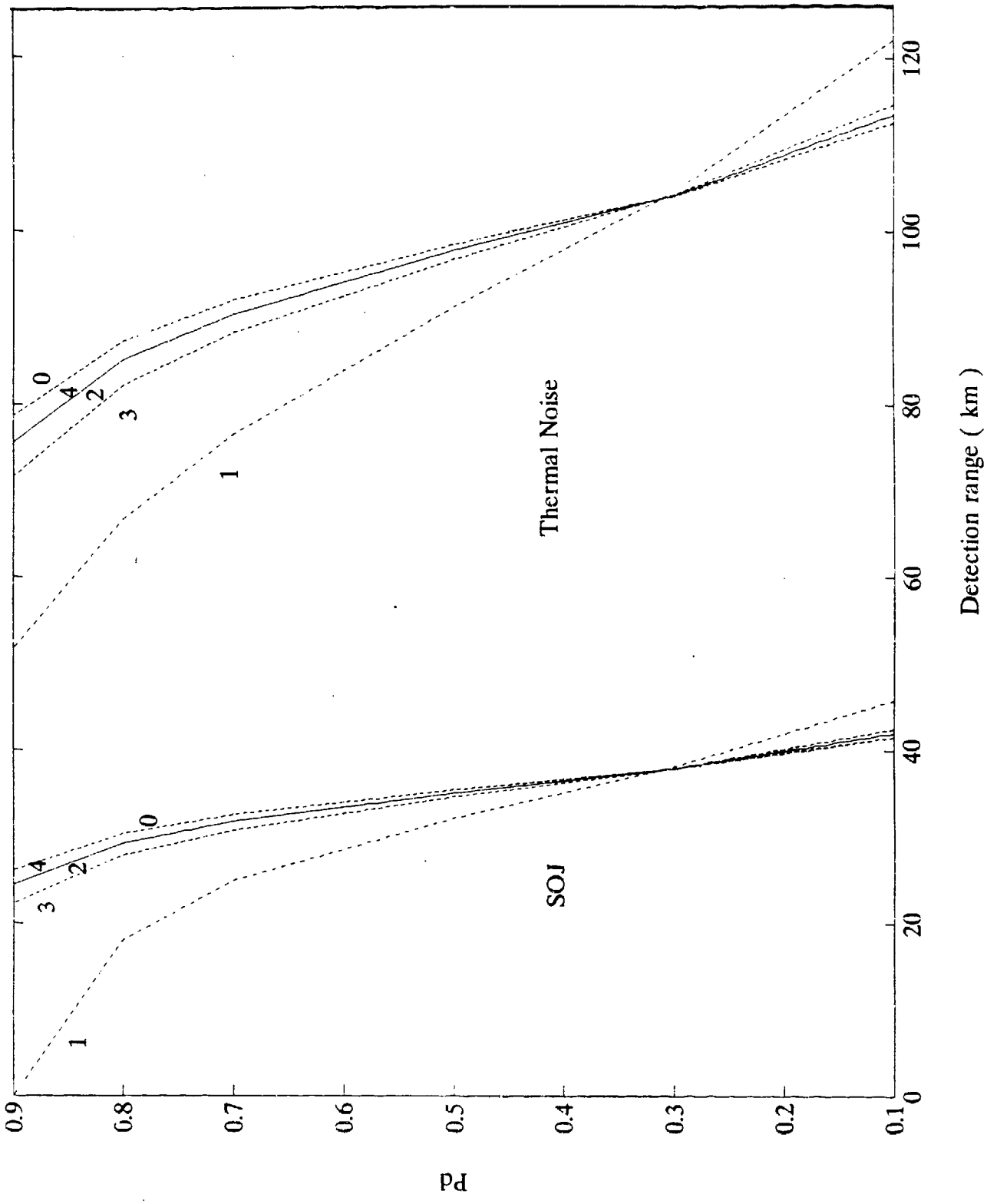

Figure 7 The comparison of detection range performance in thermal noise and SOJ

Minimum SIR required for P_d of 0.9 is 15.75 dB which can be obtained only up to range of 26.7 km (case 0). Beyond this range radar can not maintain the required SIR and thus probability of detection will go down from the required value of 0.9.

The other columns in Table 2 are defined below

J_0/N_0 is Jamming-to-noise ratio of SOJ

I_0 is Interference due to jamming

I_0/N_0 is Interference-to-noise ratio

J_0 is Jamming spectral density

E/N_o is Energy-to-noise Ratio

When radar is subjected to SOJ, the maximum radar detection range(with P_d of 0.9) is reduced from 80 km to 26.7 km as shown in Figure 7. The decrease in detection range was due to decrease in SIR. The decreased SIR was result of additional noise introduced by SOJ. However, this SOJ will not be able to affect the target detection when the target is at a distance of 26.7 km from the radar or closer. Also, as shown in Figure 7, the maximum detection range in presence of SOJ is reduced for all Swerling target models as expected.

C. DETECTION RANGE IN SURFACE CLUTTER

In this section the effect of ground clutter on SIR and maximum detection range is determined. For clutter calculations first flatland terrain type is considered.

The reflectivity of terrain is assumed to be -20 db (constant gamma model). Clutter did not make any noticeable change in SIR and in detection range.

Next mountain terrain type is considered for detection range computation. Following parameters are used in this calculation

Reflectivity	-5 dB
Clutter velocity spread	0.3 m/s
Terrain roughness	100 m
MTI improvement factor	45 dB

The last two columns in Table 3 show SIR with and without clutter. A decrease in SIR will have negative impact on the detection range.

Signal-to-interference ratio and some other parameters tabulated in Table 3 for the mountain terrain type are as follows:

C_o/N_o is the clutter to noise ratio that has already been reduced by MTI improvement factor

N_o, C_o is Noise and Clutter spectral density

$(C_o+N_o)/N_o$ is Interference to Noise Ratio

$D_x(C_o+N_o)/N_o$ is the required detectability above clutter plus noise (interference) floor

In Table 3, the ambiguous ranges are tabulated from 169.1 km to 211.2 km. The clutter has a stronger effect at close distances. Curve 1 in Figure 8 represents

clutter-to-noise ratio as a function of range. An improvement factor of 45 dB was assumed for the computation of this curve. To achieve P_d of 0.9, a detectability factor equal to 15.75 dB is required. Curve 2 represents the radar threshold to achieve P_d of 0.9. Curve 3 is target signal as function of range. The detection range for this case from Figure 8 is 85 km. It should be noted that if the improvement factor was less than 45 dB, the detection range in clutter would have been reduced.

Table 3. SIGNAL-TO-CLUTTER PLUS NOISE VS TARGET RANGE

Range	C_o/N_o	N_o	Cs_o	I_o	I_o/N_o	$D_x(C_o+N_o)/N_o$	E/N_o	SIR
22.0	15.0	-199.3	-184.3	-184.1	15.1	30.89	36.92	21.8
43.0	3.27	-199.3	-196.0	-194.3	4.9	20.70	27.31	22.4
64.0	-3.96	-199.3	-203.2	-197.8	1.5	17.22	20.07	18.6
85.1	-9.24	-199.3	-208.5	-198.8	0.5	16.24	14.06	14.1
106.1	-13.45	-199.3	-212.7	-199.1	0.2	15.94	10.22	10.0
127.1	-16.96	-199.3	-216.2	-199.2	0.1	15.84	6.52	6.4
148.1	-19.99	-199.3	-219.3	-199.2	0.0	15.79	-34.20	-34.2
169.1	17.37	-199.3	-181.9	-181.8	17.5	33.20	-90.73	-108.2
190.2	4.50	-199.3	-194.8	-193.5	5.8	21.57	-147.10	-152.9
211.2	-3.11	-199.3	-202.4	-197.6	1.7	17.48	-203.37	-205.1

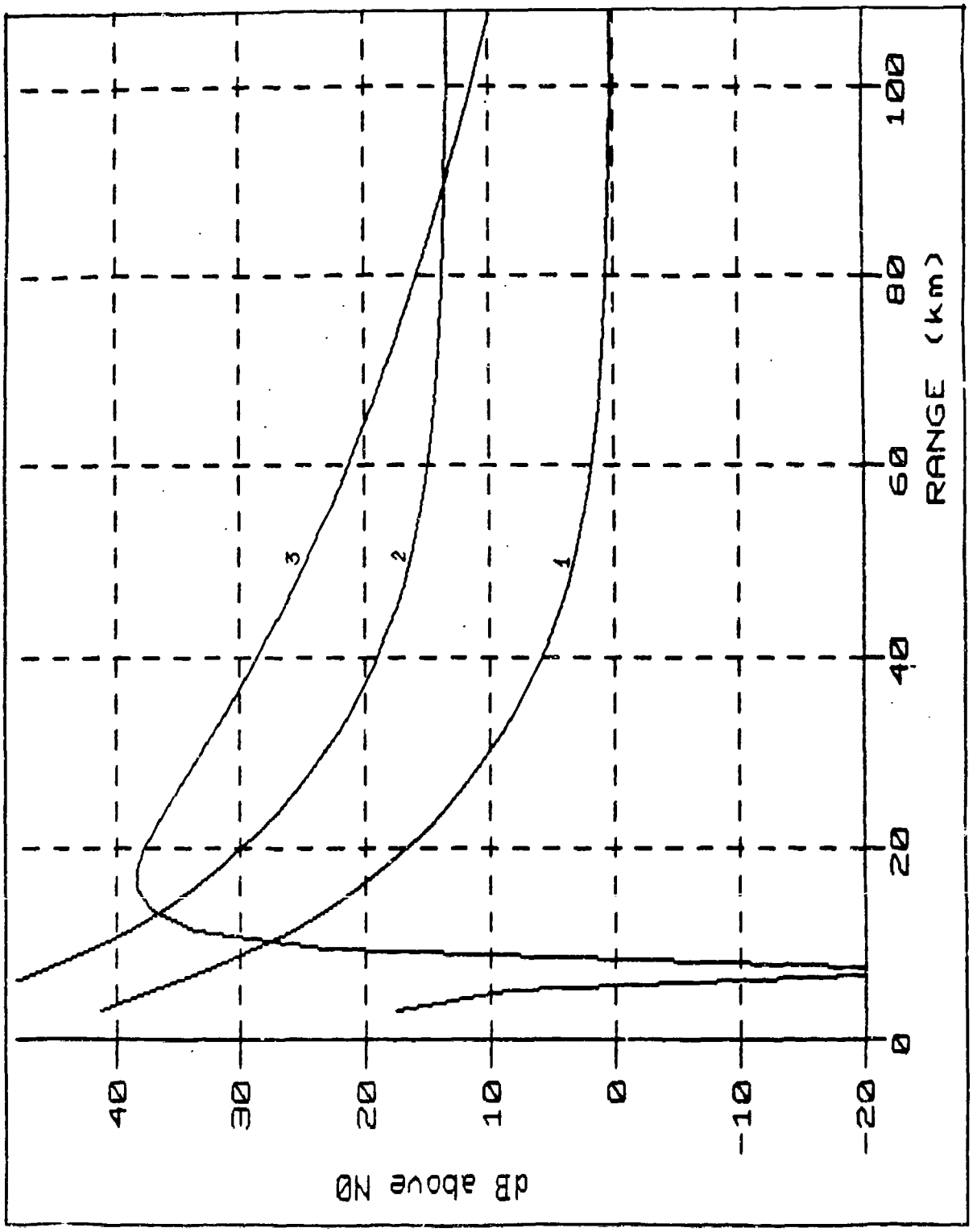

Figure 8 Signal-to-clutter plus noise ratio versus range detection for ASR-9 radar with land clutter (Mountain terrain type)

V. CONCLUSIONS AND RECOMMENDATIONS

In this thesis, radar range performance of Air Surveillance Radar ASR-9 is analyzed using a professional software package from Artech House. The basic procedure for determining the detection range is to first determine detectability factor for specific target model and required P_d and P_{fa}. The detectability factor is then used to compute the radar threshold. Target signal is determined from the given radar parameters as function of range and compared against the threshold to see if detection will take place at any of the ranges. The program was exercised to determine detection range for the following cases: thermal noise only, stand off jammer plus noise, and clutter plus noise. All five target models were considered for the cases of thermal noise and stand off jammer plus thermal noise.

The software is user friendly, but its theoretical basis is not well documented and most of formulas used in it are empirical. Software has provision to incorporate the MTI effects to counter the clutter. In Chapter III, an effort is made to mathematically describe the theory behind the program. Some parameters provided by software may not be suitable for all applications. A user can use his own data under such circumstances. For example, if the radar site is located in certain terrain that is not available in the software, the user can enter the data from other sources

instead of the data provided by the code. The software can also be used to determine jammer parameters which will deny the radar its normal coverage.

In Chapter IV, the result of performance evaluation will be used to decide if radar system performs in given condition as the desired requirement or not. Further analysis using this software has to be carried out to estimate the usefulness of the radar under varying jamming conditions such as noise quality, bandwidths, ERP, and polarization etc. Similarly, analysis has to be carried out with different terrain types such as sea, chaff, and farmland etc. Yet, analytical evaluation would not completely validate ASR-9 performance for all cases. Field test is required to evaluate its performance in the practical condition.

APPENDIX

RADAR EVALUATION SOFTWARE

The Artech House radar evaluation program is designed for use with personal computers. This program is based on the theory presented in Radar Evaluation Handbook [Ref1.]. The program predicts radar performance and determines the effect on radar performance due to changes in the parameters of the radar, target, or environment.

The theoretical basis of the program has been described in Chapter III. This program can be used to predict the detection performance of a proposed or actual radar such as ASR-9.

The radar evaluation software consists of ten modules but the modules which are related to the thesis are:

1. Radar and target description
2. Detectability factor
3. Detection range in thermal noise
4. Detection range with noise jamming
5. Detection range with surface clutter
6. Detection range with combined interference sources

A brief description of each of these modules follows.

Radar and Target Description

In this module, the major parameters of radar subsystems such as transmitter, antenna, receiver, and signal processing are entered in the program. Target parameters are also entered at this stage. Not all parameters of a subsystem are entered. For example, an average power and blind speed are computed from peak power, pulse width and PRF which have already been entered.

Radar performance is affected by the choice of radar mode. For ASR-9 radar, MTI mode is chosen. The Swerling target model and average target cross section are also selected in this module. After all entries have been completed, the file is saved for the following modules.

Detectability Factor

This program module calculates the basic detectability factor for the target model specified in Module 1, and modifies this factor for several losses resulting from receiver matching, antenna beamshape and signal processing. A mathematical background has already been given in section B of Chapter III. The program calculates the detectability factors for each value of P_d and P_{fa}. Normally, six values of P_d are given, from 0.1 to 0.9, but may be modified to include particular desired values.

False alarm time is computed from P_{fa} and other parameters in the program. Signal processing losses are provided to the software according to the type of radar. The program then calculates the detectability factor as used in equation (3.1) of Chapter III.

Detection Range in Thermal Noise

The detectability factor from the previous module is used to compute maximum detection range in thermal noise. Entries in this module include clear-air attenuation, precipitation attenuation, noise spectral density, the receiving line loss and pattern-propagation factor. The program calculates the detection range, signal energy and SNR for each probability of detection. The file in this module will be used later in the jamming module.

Detection Range with Noise Jamming

The user specifies the jammers and their type such as stand-off jammer, escort jammer and self screening jamming. The program calculates jamming plus thermal noise density as a function of target range. It also calculates pattern-propagation factor in the direction of jammer and its equivalent jammer noise temperature.

Detection Range with Surface Clutter

A land or sea clutter environment can be specified. Clutter parameters may be entered directly by the user, or accepted from standard models stored in the program. For clutter rejection, a clutter improvement factor is entered or is

computed from previous inputs. If the factor is calculated by program, it may vary with range and probability of detection. The program calculates the ratios of interference-to-noise, signal-to-noise and signal-to-interference as a function of target range for each detection probability. It also computes the clutter RCS and pattern propagation factor for each terrain type in the first two range ambiguities.

Detection Range with Combined Interference

This module combines the effects of thermal noise, jamming, volume clutter and surface clutter. Graphical procedure is most convenient to use for determination of detection range for the most general case and Artech House software employs the graphical procedure. Plots of signal and interference level versus range are generated in section C of Chapter IV.

Radar Evaluation Software has several other modules which have not been used in this thesis.

LIST OF REFERENCES

1. David, K., Barton, Charles, E.,Cook, and Paul Hamilton, *Radar Evaluation Handbook*, Artech House, 1991.

2. David, K., Barton, *Modern Radar System Analysis*, Artech House, 1988.

3. David, K., Barton, Radar, Artech House, Vol.2, 1974.

4. D. Curtis Schleher, *Introduction to Electronic Warfare*, Artech House, 1986.

5. Merill, I., Skolnik, *Introduction to Radar Systems*, Mcgraw-Hill, 1962.

6. Paul, A., Lynn, *Radar Systems*, Van Nostrand Reinhold, 1987.

7. George, W., Stimson, *Introduction to Airborne Radar*, Hughes Aircraft, 1983.

8. M.L. Stone and J.R. Anderson, Advances in Primary-Radar Technology, The Lincoln Laboratory Journal, Vol.2, No.3, 1989, pp.363-380.

9. David, K., Barton, *Land Clutter models for radar design and analysis*, Proc.IEEE 73, No.2, February 1985, pp.198-204.

10. G.V. Trunk, *Radar Properties of Non-Rayleigh Sea Clutter*, IEEE Transaction on Aerospace and Electronic Systems, March 1972, pp.196-204.

11. Fred, E., Nathanson, *Radar Design Principles*, Mcgraw-Hill, 1990.

INITIAL DISTRIBUTION LIST

1. Defense Technical Information Center Cameron Station Alexandria, Virginia 22304-6145	2
2. Library, Code 52 Naval Postgraduate School Monterey, California 93943-5000	2
3. Professor Jeffrey Knorr, Chairman, Code EW Electronic Warfare Academic Group Naval Postgraduate School Monterey, California 93943-5000	1
4. Dr. Gurnam Gill, Code EC/GL Department of Electrical and Computer Engineering Naval Postgraduate School Monterey, California 93943-5000	3
5. Dr. David C. Jenn, Code EC/JN Department of Electrical and Computer Engineering Naval Postgraduate School Monterey, California 93943-5000	1
6. LT. Amnauy Thongrod 35 Soi Sanam klee, Lumpinee Patumwon, Bangkok 10330 Thailand	1